Controlling Kinesin by Reversible Disulfide Cross-linking: Identifying the Motility-producing Conformational Change✪

Michio Tomishige and Ronald D. Vale

The Howard Hughes Medical Institute and the Department of Cellular and Molecular Pharmacology, University of California, San Francisco, California 94143

Abstract. Conventional kinesin, a dimeric molecular motor, uses ATP-dependent conformational changes to move unidirectionally along a row of tubulin subunits on a microtubule. Two models have been advanced for the major structural change underlying kinesin motility: the first involves an unzippering/zippering of a small peptide (neck linker) from the motor catalytic core and the second proposes an unwinding/rewinding of the adjacent coiled-coil (neck coiled-coil). Here, we have tested these models using disulfide cross-linking of cysteines engineered into recombinant kinesin motors. When the neck linker motion was prevented by cross-linking, kinesin ceased unidirectional movement and only showed brief one-dimensional diffusion along microtubules. Motility fully recovered upon adding reducing agents to reverse the cross-link. When the neck linker motion was partially restrained, single kinesin motors showed biased diffusion towards the microtubule plus end but could not move effectively against a load imposed by an optical trap. Thus, partial movement of the neck linker suffices for directionality but not for normal processivity or force generation. In contrast, preventing neck coiled-coil unwinding by disulfide cross-linking had relatively little effect on motor activity, although the average run length of single kinesin molecules decreased by 30–50%. These studies indicate that conformational changes in the neck linker, not in the neck coiled-coil, drive processive movement by the kinesin motor.

Key words: kinesin • processivity • disulfide cross-linking • neck linker • one-dimensional diffusion

Introduction

Conventional kinesin (herein referred to as kinesin) is a microtubule-based motor protein that is involved in transporting membranous organelles and intermediate filaments within cells (Hirokawa, 1998; Goldstein and Philp, 1999). Kinesin, a dimeric protein with two motor heads and a tail domain that docks onto a cargo, is a highly processive motor capable of taking ~150 steps of 8-nm length along a microtubule before dissociating (Howard et al., 1989; Block et al., 1990; Svoboda et al., 1993; Hackney, 1995; Vale et al., 1996; Gilbert et al., 1998). Processivity is an important biological adaptation that enables one or a relatively small number of kinesin molecules to transport cargo within the cell.

Understanding the mechanism of kinesin motility has been aided by structural studies of the kinesin motor domain. Three-dimensional crystal structures of kinesin monomers and a short dimer have revealed several domains important for the motor function (Kull et al., 1996; Sack et al., 1997; Kozielski et al., 1997) (see Fig. 1 a). The NH$_2$-terminal ~320 amino acids (a.a.),[1] which are conserved throughout the kinesin superfamily, form a compact globular domain (termed the catalytic core) that contains the microtubule binding and ATP hydrolysis sites. Emerging from the COOH terminus of the catalytic core is the neck region (Vale and Fletterick, 1997), which consists of two different parts: the ~15 a.a. "neck linker" (see Fig. 1 a, red), which can interact with the catalytic core, and the subsequent ~30 a.a. "neck coiled-coil" (see Fig. 1 a, cyan). In the dimeric kinesin crystal structure (Kozielski et al., 1997), the catalytic cores cannot both bind simultaneous to two adjacent binding sites on a microtubule protofilaments (separated 8 nm apart). Since a two-head–bound intermediate is thought to be critical for processive motion (Vale and Milligan, 2000), it is thought that some

---

[1]*Abbreviations used in this paper*: a.a., amino acid; AMPPNP, 5'-adenylylimidodiphosphate; DTNB, 5,5'-dithiobis-(2-nitrobenzoic acid); GFP, green fluorescent protein; MSD, mean-square-displacement; NEM, *N*-ethylmaleimide; oPDM, *N,N*'-1,2-phenylenedimaleimide; pPDM, *N,N*'-1,4-phenylenedimaleimide.

element in the dimeric kinesin crystal structure must melt during the enzymatic cycle (Block, 1998). Two theories have been advanced for this conformational change: the first involves an "unzippering" of the neck linker from the catalytic core (Romberg et al., 1998) and the second proposes a partial "unwinding" of the neck coiled-coil (Tripet et al., 1997; Hoenger et al., 1998).

In favor of the neck linker peeling model, Rice et al. (1999) have detected ATP-dependent conformational change of the neck linker using electron paramagnetic resonance, fluorescence resonance energy transfer, and cryo-EM. The neck linker is docked onto the catalytic core when kinesin is bound to the microtubule and ATP is in the active site, but becomes unzipped in the ADP or nucleotide-free state. These findings, together with cryo-EM work that reveals the docking orientation of kinesin on the microtubule, suggest that the two kinesin heads can span the distance between tubulin binding sites if the neck linker of the rear head is docked and pointing forward and the neck linker on the forward head is detached and pointing backward (Vale and Milligan, 2000). Further supporting an important role of the neck linker in motility, Case et al. (2000) replaced the neck linker with a random coil structure and found a 450-fold decrease in motor velocity.

An alternative model proposes that the key structural change in kinesin motility is the unwinding and rewinding of the first half of the neck coiled-coil (Tripet et al., 1997; Hoenger et al., 1998, 2000; Mandelkow and Johnson, 1998). In favor of this model is the fact that the first half of the neck coiled-coil (residues 337–353) contains nonideal residues that destabilize the coiled-coil structure, while the latter half of the coiled-coil (354–368) is supported by more stable interactions (Tripet et al., 1997; Thormahlen et al., 1998). Furthermore, when Hoenger et al. (2000) prevented the unwinding of the neck coiled-coil through an engineered disulfide bridge at the beginning of the structure, they reported a 13-fold increase in K_m(MT), which they interpreted as due to a loss in processivity. On the other hand, Romberg et al. (1998) showed that replacing kinesin's native neck coiled-coil with a highly stable artificial coiled-coil did not greatly reduce processivity, suggesting that the neck coiled-coil unwinding is not essential for kinesin motility. However, the interpretation by Romberg et al. was criticized on the basis that a partial unwinding of the coiled-coil may have been still possible in the stable coiled-coil mutant (Mandelkow and Hoenger, 1999).

To test these two models for kinesin's processivity, we engineered disulfide bridges in the neck linker or the neck coiled-coil to prevent potential conformational changes in these regions. The effect of cross-linking on the motor functions was assayed by ATPase assays, multiple motor motility assays, and single molecular motility assays. Cross-linking of the neck coiled-coil had little effect on kinesin processivity, whereas cross-linking of the neck linker disabled processive movement. Kinesin cross-linked at the middle position of the neck linker showed a small degree of directional motion, suggesting that partial movement of the neck linker is sufficient for directionality but not for processivity. Our results provide functional proof for the model in which dynamic motions of the neck linker, but not the neck coiled-coil, drive kinesin's mechanochemical cycle.

Materials and Methods

Cloning and Protein Purification

As a template for mutagenesis, we used a human 560–amino acid kinesin whose solvent exposed cysteines were mutated to Ser/Ala (C7S/C65A/C168A/C174S/C294A/C330S/C421A) (Rice et al., 1999); fused COOH-terminal to this "Cys-light K560" was the green fluorescent protein (GFP; Phe64Leu/Ser65Thr variant) followed by a six-histidine tag. For making a monomeric construct, we used a 339–amino acid Cys-light kinesin fused to GFP. Ideal locations for introducing cysteines for disulfide bond formation were determined using the program SSBOND (Hazes and Dijkstra, 1988). Cysteines were introduced into these constructs using a protocol involving QuickChange mutagenesis (Stratagene) followed by subsequent subcloning in a pET17b vector (Novagen, Inc.), as previously described (Case et al., 1997). The sequences of all constructs were verified. *Escherichia coli* BL21 (DE3) was transformed with the expression plasmid construct, and protein expression was induced as described previously (Case et al., 1997; Romberg et al., 1998), except that cells were collected and lysed at pH 6.0 to prevent disulfide cross-linking and the pH of supernatants was raised to 8.0 just before binding to Ni-NTA resin. Kinesin proteins were purified by Ni-NTA chromatography (QIAGEN) followed by HiTrap-Q ion exchange chromatography (Amersham Pharmacia Biotech) as described (Case et al., 1997; Romberg et al., 1998). To remove inactive motor proteins, kinesin was finally purified by microtubule affinity (Case et al., 1997). In brief, proteins were incubated with ∼1.5 mg/ml taxol-stabilized microtubules and 1 mM AMPPNP and centrifuged over a glycerol cushion (200,000 *g* for 10 min). Active kinesin motors were released from the microtubule in 12 mM Pipes buffer (pH 6.8) containing 200 mM KCl, 5 mM ATP, 5 mM MgCl₂, 2 mM EGTA, and 20 μM taxol. DTT in the protein solution also was removed in this step. Immediately after microtubule affinity purification, motors were assayed or were frozen with 10% sucrose added and stored in liquid nitrogen. Protein concentration was quantitated using SDS-PAGE as described previously (Woehlke et al., 1997).

Chemical Cross-linking

Thiol-specific reagents were obtained from Sigma-Aldrich (5,5'-dithiobis-(2-nitrobenzoic acid) [DTNB], DTT, *N*-ethylmaleimide [NEM]; *N,N'*-1,2-phenylenedimaleimide [oPDM]; *N,N'*-1,4-phenylenedimaleimide [pPDM]). DTNB was dissolved in DMSO at 100 mM concentration, oPDM and pPDM were dissolved in acetonitrile at 10 mM concentration and the solutions were stored at 4°C. DTT and NEM solutions were prepared freshly by dissolving in assay buffers. Assay buffers used were either BRB12 (12 mM Pipes [pH 6.8], 2 mM MgCl₂, 1 mM EGTA; for ATPase assay and single molecule motility assay) or BRB80 (80 mM Pipes [pH 6.8], 2 mM MgCl₂, 1 mM EGTA; for multiple motor assay and optical trapping bead assay). Disulfide bonds were reversibly formed by oxidation using DTNB. Bifunctional thiol reagents oPDM and pPDM were used to cross-link two thiols with different lengths, and the monofunctional thiol reagent NEM was used for monovalent modification of a thiol. Reactions were carried out by adding 200 μM thiol-specific reagents (DTNB, oPDM, pPDM, or NEM) to 0.5–1 μM kinesin and incubation at 4°C overnight. Control reactions were carried out in parallel by adding equal amount of buffer (for Cys337, Cys344, and Cys337/Cys344 constructs) or 1 mM DTT (for Cys330/Cys4 and Cys334/Cys222 constructs). Unreacted oPDM or pPDM were quenched by the addition of 10 mM 2-mercaptoethanol. Unreacted NEM was quenched by the addition of 5 mM DTT for the ATPase assay; otherwise it was diluted or removed using a flow cell for the motility assays. For a control, disulfide-bond formation was reversed by incubation of DTNB-treated motor with 5 mM DTT at 4°C for more than 3 h. Disulfide or chemical cross-linking was verified by adding SDS sample buffer without reducing reagents followed by SDS-PAGE (4–12% polyacrylamide) and Coomassie blue staining.

ATPase and Microtubule-gliding Assays

Microtubule-stimulated ATPase activities were measured using a spectrophotometer with a coupled enzymatic assay as described (Woehlke et al., 1997) except that DTT was not added. Reactions contained 40–100 nM kinesin, varying concentrations of microtubules (0–12 μM for dimeric and 0–40 μM for monomeric constructs), and 1 mM MgATP in BRB12 buffer. Multiple motor motility assays were performed using rhodamine-labeled microtubules and fluorescence microscopy in flow cells as described (Woehlke et al., 1997) except that 2-mercaptoethanol was not added to the

assay buffer. Anti-GFP antibodies were used to bind and orient the motor on the surface of the coverslip. The gliding velocity of microtubules over the motors was measured based on the distance travelled during 30–60 s.

Single Motor Motility Assays

Individual GFP-kinesin fusion molecules moving along sea urchin sperm flagellar axonemes were visualized in a custom-built total internal reflection fluorescence microscope as described previously (Pierce and Vale, 1998, 1999; Romberg et al., 1998). The assay solution contained ~1 nM kinesin-GFP, 2.5 mg/ml casein, an oxygen scavenging system (without 2-mercaptoethanol) (Pierce and Vale, 1998), 1 mM MgATP, and Cy5-labeled axonemes in BRB12 buffer. GFP molecules were illuminated with an argon laser (488 nm) at 5 mW. The fluorescent images of both axonemes and GFP molecules were recorded onto a S-VHS tape after four-frame averaging. The images were digitized (10 or 15 frames/s) and analyzed on a computer using custom macros in the program NIH image. The observed run lengths, velocities, and association times of moving fluorescent spots along axonemes were measured as described (Romberg et al., 1998; Shimizu et al., 2000). The distributions of run length and association time were fitted with exponential curves ($C \cdot \exp[-x/\lambda]$, where λ is the average run length) (Romberg et al., 1998), except for the distributions of run length of DTNB-treated Cys330/Cys4 and Cys334/Cys222 that were fitted based on Gaussian distributions ($C \cdot \exp[-\{x-x_d\}^2/2\sigma^2]$, where x_d is the average net displacement toward plus end). Positions of the fluorescent spot undergoing Brownian diffusion were determined using a macro program provided by Dr. Y. Inoue (University of Tokyo, Tokyo, Japan). The accuracy of position determination of individual GFP spots was ~30 nm, which was estimated as the standard deviation of positions of the spots bound onto axonemes in the presence of 1 mM AMPPNP.

Optical Trapping Bead Assays

Kinesin-GFP molecules were coupled with latex beads via affinity-purified anti-GFP antibodies. 15 mg of 1-ethyl-3-(3-dimethlaminoprophyl) carbodiimide (EDAC; Molecular Probes) and 15 mg of N-hydroxysulfosuccinimide (Molecular Probes) were added to 50 µl of 1-µm carboxylate-modified latex beads (10% solid; Bangs Laboratories) in 20 mM MES (pH 6.0) containing 100 mM NaCl, and mixed on a shaker for 30 min at room temperature. After four washes by centrifugation and resuspension, the pellet was resuspended in 300 µl of 0.1 M sodium phosphate buffer (pH 7.0) containing 100 µg anti-GFP antibodies and 1 mg/ml BSA. After mixing for 2 h at room temperature, beads were washed four times, and resuspended in 0.1 M sodium phosphate buffer (pH 7.0) containing 0.1% NaN₃ and 4 mg/ml BSA, and stored at 4°C. Kinesin-GFP dilution was mixed with the beads for 20 min at 4°C, and further diluted in assay solution containing 1 mM MgATP, 0.5 mg/ml casein, the oxygen scavenging system (without 2-mercaptoethanol) in BRB80 buffer (Coppin et al., 1997). Kinesin-coated beads were captured and interacted with rhodamine-labeled sea urchin sperm flagellar axonemes using an optical trap, and the motility of the bead along an axoneme under load was assayed as described previously (Coppin et al., 1997). Trap stiffness was calibrated as described (Coppin et al., 1997) and was 0.029 pN/nm in these experiments. Trapped beads were brought into contact with an axoneme and held for more than 90 s. When the bead moved, the displacement of the bead was acquired at 2 kHz. Force–velocity curves and dissociation rates were obtained as described previously (Coppin et al., 1997), except that they were not corrected for the compliance of the motor–bead linkage, therefore the velocity in the force–velocity curve is slightly underestimated (~10%). K560-GFP molecules tended to dissociate from axonemes before reaching a stall plateau, which causes a biased sampling of velocities at high forces. To compensate for this bias, the motors that dropped out were assumed to have zero velocity at higher loads (Coppin et al., 1997). This correction significantly shifted the curves to the left (i.e., lower forces). True curves are expected to lie between the corrected and uncorrected curves.

Online Supplemental Material

The online version of this article contains QuickTime movies that accompany Fig. 3, which better visualize the dramatic changes in the movement of kinesin after neck linker cross-linking. Videos 1 and 2 show the movements of Cys330/Cys4 molecules under reduced and oxidized conditions, respectively. The image of an axoneme is displayed first, followed by the images of single kinesin-GFP molecules moving along axonemes visualized by total internal reflection fluorescence microscope. The times (in seconds) are shown in the upper right of the movies and are 3× real

speed. Online supplemental material available at http://www.jcb.org/cgi/content/full/151/5/1081/DC1.

Results

Cross-linking of Kinesin's Neck Linker

A 560–amino acid kinesin whose solvent-exposed cysteines were replaced by either Ser or Ala (Rice et al., 1999) was used as a template for introducing pairs of cysteine residues for reversible disulfide cross-linking. This "Cys-light K560" protein (also designated "WT" in this paper) exhibited identical ATPase activity and processive motility to K560, but avoided potential deleterious effects associated with oxidation of surface cysteines. The program SSBOND identified only two pairs of residues in the neck linker whose Cα–Cα and calculated Cβ–Cβ distances are capable of forming energetically favorable disulfide bonds (Fig. 1 a): (a) between residue 334 at the end of the neck linker and residue 222 at the tip of the catalytic core; and (b) between residue 330 (located between β9 and β10) and residue 4 at the NH₂ terminus. A disulfide bond between residues 334 and 222 would be expected to totally immobilize the ATP-dependent neck linker movement, while a disulfide bond between residues 330 and 4 should partially immobilize the neck linker movement.

Cys334/Cys222 and Cys330/Cys4 constructs were prepared, the expressed proteins were purified from bacteria, and disulfide bond formation after oxidation with DTNB (5,5'-dithio-bis[2-nitrobenzoic acid]) was examined using SDS-PAGE under non-reducing conditions. Both neck linker mutants displayed small electrophoretic mobility changes after oxidation (Fig. 1 b); with intermediate

Table I. Effect of Neck Cross-linking on ATPase Activity and Microtubule Gliding Velocity

Construct	DTNB*	ATPase‡		MT velocity§
		k_{cat}	K_m (MT)	
		ATP/s per head	µM tubulin	µm/min
WT	−	31.9 ± 4.9	1.01 ± 0.34	17.0 ± 2.5
	+	29.5 ± 6.1	1.27 ± 0.32	17.3 ± 2.4
C334/C222	−	13.2 ± 2.1	0.62 ± 0.35	6.9 ± 4.6
	+	6.8 ± 3.2	2.36 ± 2.40	1.2 ± 1.2
	NEM	12.2 ± 6.0	1.51 ± 1.99	9.3 ± 4.0
C330/C4	−	19.8 ± 3.1	0.57 ± 0.47	8.2 ± 2.7
	+	9.9 ± 3.3	2.35 ± 2.84	2.5 ± 1.8
	NEM	19.5 ± 2.1	0.45 ± 0.17	7.1 ± 2.9
C344	−	19.2 ± 1.5	0.84 ± 0.75	15.4 ± 5.5
	+	20.9 ± 3.9	1.24 ± 0.67	14.1 ± 4.9
C337	−	20.0 ± 4.3	1.20 ± 1.03	12.8 ± 4.1
	+	18.9 ± 1.2	1.59 ± 1.28	9.0 ± 3.2
C337/C344	−	25.8 ± 5.4	1.19 ± 0.82	22.4 ± 5.5
	+	26.6 ± 2.7	1.51 ± 0.40	18.7 ± 5.0

Microtubule-stimulated ATPase and microtubules gliding assays were performed using K560 Cys-light mutants as described in Materials and Methods.
*Disulfide crosslinking was performed by incubation of the constructs with DTNB (− and + indicate without and with 200 µM DTNB). NEM indicates control reaction (monovalent modification) with 1 mM NEM.
‡Maximal ATP turnover rates k_{cat} and apparent Michaelis-Menten constants K_m (MT) were determined by the best fit to a hyperbolic curve of 8–10 ATP turnover rates at varying microtubule concentrations. Mean ± SD values were obtained from four independent assays using two different protein preparations.
§Mean microtubule gliding velocities were obtained from >50 microtubule measurements. Also see Figs. 2 a and 4 a for distributions.
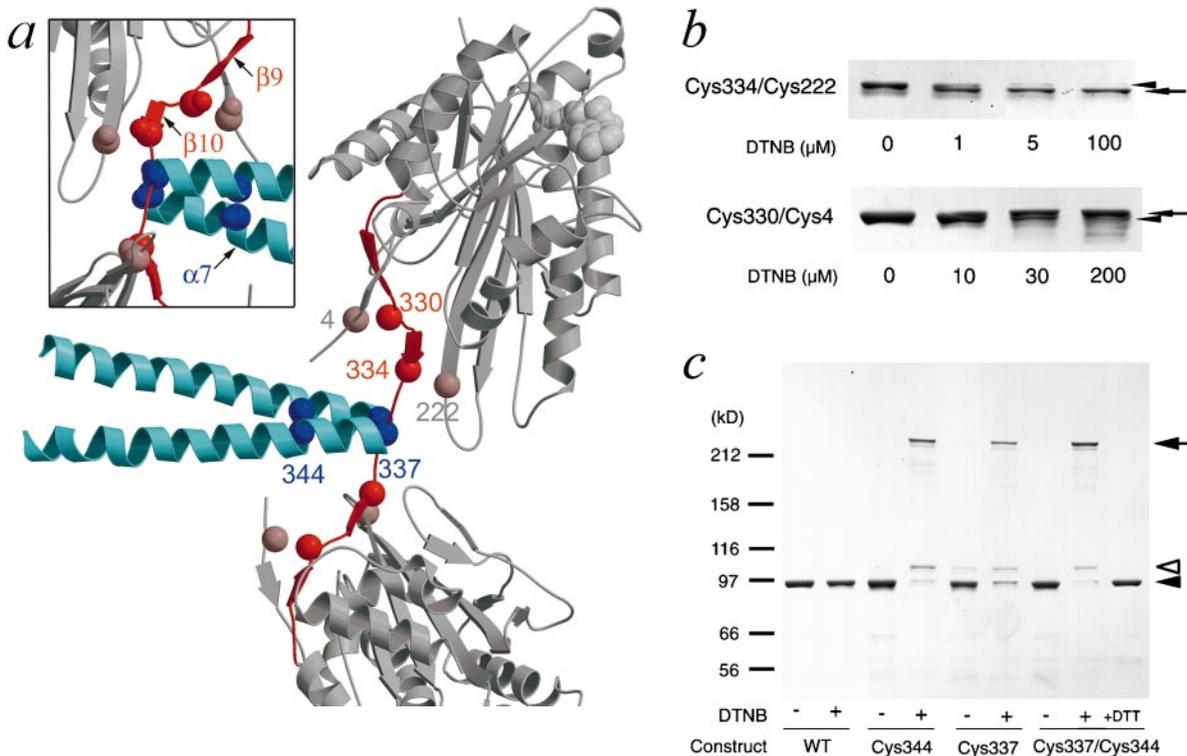
Figure 1. Constructs for cross-linking of the neck region. (a) Three-dimensional structure of rat kinesin dimer (PDB No. 3KIN [Koziel-ski et al., 1997]; numbered as in human kinesin). The catalytic core (residues 2–322; gray), the neck linker (residues 323–336; red) and the neck coiled-coil (337–368; cyan) are shown. Positions of the mutations for cross-linking are shown by space filing of Cα atoms (Ser330Cys/Leu4Cys or Glu334Cys/Lys222Cys for cross-linking of the neck linker and Ala337Cys or Tyr344Cys for cross-linking of the neck coiled-coil). Inset shows a view from the reverse side. Smaller spheres indicate positions of Cβ atoms. (b) DTNB-induced disulfide cross-linking of neck linker mutants (Cys334/Cys222 and Cys330/Cys4), and (c) neck coiled-coil mutants (Cys344, Cys337, Cys337/Cys344) as analyzed by nonreducing SDS-PAGE. The DTNB concentration in c was 200 μM. Disulfide formation was reversed by subsequent treatment with 5 mM DTT (+DTT, right lane in c). The arrowheads show noncross-linked kinesin and the arrows show intramolecular cross-linked kinesin (b) and intermolecular cross-linked kinesin (c). The intramolecular cross-link for C334/C222 produces an increase in electrophoretic mobility, whereas the C330/C4 cross-link decreases mobility. No higher molecular weight band (i.e., intermolecular cross-linking) was detected for the neck linker mutants (not shown). The band indicated by open arrowhead (c) may represent a modified monomer or a dimer of degradation products.

DTNB concentrations, two bands (noncross-linked and cross-linked proteins; arrowheads and arrows in Fig. 1 b, respectively) were discernible. The mobility of the WT protein (Cys-light K560) was not affected by the oxidative treatment (Fig. 1 c).

Cys334/Cys222 and Cys330/Cys4 mutants were assayed under reducing and oxidizing conditions for microtubule-stimulated ATPase rates to determine whether neck linker cross-linking affects basic enzymatic functions (Table I). Under reducing conditions, the k_{cat} for microtubule-stimulated ATPase (13.2 and 19.8 ATP/s per head for Cys334/Cys222 and Cys330/Cys4, respectively) was lower than WT (31.9 ATP/s per head). The K_m(MT), however, was within twofold of WT. After oxidative cross-linking, k_{cat} decreased by an additional ~50% and the K_m(MT) increased by approximately fourfold for both constructs. Addition of the monovalent thiol-reactive reagent NEM, on the other hand, did not affect the ATPase properties of Cys334/Cys222 and Cys330/Cys4. These results indicate that disulfide bond formation in the neck linker, and not cysteine modification per se, affects kinesin's enzymatic activity.

The almost precise 50% decrease in k_{cat} in both constructs after oxidative cross-linking was striking. One possible explanation was that only one head of the kinesin dimer was enzymatically activated by an encounter with the microtubule, perhaps because the second head was restrained from reaching another tubulin subunit by neck linker cross-linking (see Fig. 6, b and c). Alternatively, cross-linking could simply cause a twofold decrease in the enzymatic activity of the catalytic core. We tested these possibilities by preparing a Cys-light monomeric kinesin (K339-GFP; Case et al., 2000) with cysteines introduced at residues 330 and 4 for neck linker cross-linking. After oxidative cross-linking, the k_{cat} of this neck cross-linked monomer decreased by only 8% (from 27.7 ± 4.0 to 25.6 ± 3.4 ATP/s per head), and the K_m(MT) increased only slightly from 10.6 ± 3.9 to 14.2 ± 4.5 μM tubulin. This result suggests that the 50% decrease in k_{cat} of the dimer after cross-linking is not due to an alteration of the catalytic mechanism but due to an inability of both heads to access the microtubule.

The effect of neck linker cross-linking on kinesin dimer-induced microtubule gliding (a multiple motor motility assay) was even more dramatic than its effect on enzymatic activity (Fig. 2 a and Table I). In the presence of reduced Cys334/Cys222, virtually all microtubules moved smoothly and unidirectionally. The distribution of velocities was broad and the mean velocity was twofold lower than WT
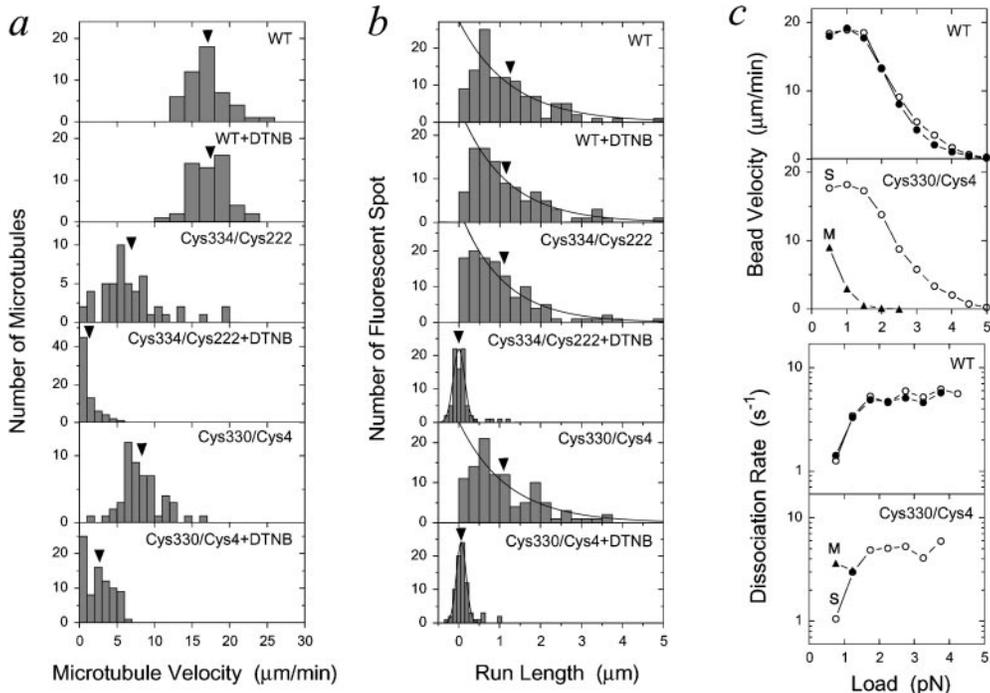
Figure 2. Effects of neck linker cross-linking on kinesin motility. WT denotes K560 Cys-light kinesin without cysteine introduction. (a) Histograms of microtubule gliding velocities without and with DTNB treatment are shown. Arrowheads indicate mean value (Table I). (b) Histograms of run lengths of single molecular motility of neck linker cross-linked kinesins along axonemes visualized using total internal reflection fluorescent microscopy. The distributions were fitted with either an exponential curve or a Gaussian curve (see Materials and Methods). Arrowheads indicate the average run length (Table II). (c) Load-dependent velocity and dissociation rate of WT and Cys330/Cys4 molecules were determined by optical trapping beads assays. (Open circle) Without DTNB; (closed circle) with DTNB; (triangle) with DTNB at 10 times higher motor density (also marked with "M" to differentiate this multiple motor condition from single motor conditions ["S"]). Force–velocity curves shown here represent a lower bound for force production (see Materials and Methods).

(Fig. 2 a). However, under oxidizing conditions, the majority of microtubules were attached to the kinesin-coated surface but showed very slow or undetectable movement (<1 μm/min). Many of the moving microtubules were also bent (data not shown), which could be explained if one or a few noncross-linked molecules moved a microtubule while inactive cross-linked motors attached to the same microtubules created resistance (Gittes et al., 1996). In contrast, oxidized Cys330/Cys4 moved the majority of microtubules at a very slow velocity of 2.5 μm/min (Fig. 2 a), which is similar to that reported for a monomeric Cys-light kinesin (2.4 μm/min; Rice et al., 1999). Thus, oxidized Cys330/Cys4 displays greatly reduced unidirectional motile activity, while oxidized Cys334/Cys222 possesses no or extremely limited motile activity.

To elucidate the effect of neck linker cross-linking on processive movement, single molecule movements were observed using total internal reflection fluorescence microscopy (Vale et al., 1996) using GFP-tagged kinesin proteins (Pierce and Vale, 1999). Under reducing conditions, Cys334/Cys222 and Cys330/Cys4 moved smoothly and unidirectionally and displayed run lengths and velocities similar to WT (Fig. 2 b and Table II) (also see online supplemental movie). After oxidative treatment with DTNB, binding of individual molecules to axonemes were still observed at a similar frequency to that observed under reducing conditions (Table II), but the molecules dissociated rapidly without displaying unidirectional smooth movements. The association time decreased six- and ninefold for Cys334/Cys222 and Cys330/Cys4 after DTNB treatment, respectively (Table II). When the oxidized mutants were treated with >10-fold excess of DTT over DTNB, the molecules again showed unidirectional motion along

axonemes with similar velocities and run lengths to that before oxidation (Table II, +DTT). Thus, the inhibition of processive motility was completely reversible. Monovalent modification using NEM did not affect the velocity and run length (Table II, NEM), indicating that cysteine modification per se does not affect processive motion. These results demonstrate that neck linker cross-linking disables the processive movement of the kinesin dimer.

Unexpectedly, oxidized neck linker molecules showed one-dimensional diffusion along the axonemes (see online supplemental movie). Similar random diffusional motion restricted to the longitudinal axes of microtubules was previously described for some molecular motors and postulated to involve a weak interaction between the motor and the microtubule (Vale et al., 1989; Okada and Hirokawa, 1999). Displacements could not be accurately detected for molecules that dissociated within 0.5 s, but were apparent for molecules that remained bound to the axoneme for longer periods of time (Fig. 3 a). The net displacements of oxidized Cys334/Cys222 displayed a Gaussian distribution centered on zero (Fig. 2 b and Table II). The mean-square-displacements (MSD; Chandrasekhar, 1943) also increased linearly with time (Fig. 3 b), indicating that the motion of this cross-linked mutant was diffusional (diffusion coefficient of 2.4×10^{-11} cm^2/s) and did not contain a directed component. These results cannot be explained by a bidirectional motion with occasional switching of the direction (Endow and Higuchi, 2000), since the MSD-Δt plot would deviate from linearity at shorter time scale, which was not observed. In contrast, cross-linked Cys330/Cys4 exhibited a small bias in the diffusional motion towards the microtubule plus end (Fig. 3 a), as evidenced by the slight offset in the Gaussian distribution of net displace-

Table II. Effect of Neck Cross-linking on Single Molecule Motility

| Construct | DTNB* | Velocity[‡] | Run Length[§] | | Association time[‖] | Frequency[¶] |
			Observed	Corrected		
		(μm/min)	*(μm)*	*(μm)*	*(sec)*	*(/min/μm/nM)*
WT	−	20.2 ± 4.0	1.26 ± 0.15	1.83	3.6 ± 0.4	1.3
	+	20.2 ± 4.1	1.13 ± 0.07	1.56	3.2 ± 0.4	1.1
C334/C222	−	20.6 ± 5.1	1.07 ± 0.07	1.36	2.5 ± 0.2	2.9
	+	0.0[‡]	0.00 ± 0.02	0.00	0.4 ± 0.05	2.4
	+DTT	19.0 ± 4.2	1.29 ± 0.19	1.71	2.8 ± 0.4	2.9
	NEM	21.2 ± 4.0	1.21 ± 0.14	1.57	2.7 ± 0.4	2.1
C330/C4	−	22.2 ± 5.7	1.19 ± 0.14	1.63	3.1 ± 0.4	2.2
	+	2.4[‡]	0.06 ± 0.01	0.07	0.3 ± 0.03	2.7
	+DTT	18.5 ± 4.6	1.12 ± 0.13	1.63	3.7 ± 0.5	2.3
	NEM	21.0 ± 4.6	1.04 ± 0.08	1.39	2.9 ± 0.3	3.0
C344	−	20.0 ± 5.6	1.04 ± 0.07	1.43	3.2 ± 0.4	2.0
	+	22.6 ± 4.9	0.80 ± 0.09	1.05	2.7 ± 0.3	1.9
	+DTT	21.7 ± 4.3	1.08 ± 0.17	1.54	3.5 ± 0.4	2.0
C337	−	19.7 ± 3.4	1.08 ± 0.09	1.51	3.3 ± 0.6	2.4
	+	19.4 ± 4.4	0.70 ± 0.06	0.86	2.2 ± 0.1	2.4
	+DTT	21.0 ± 5.0	1.34 ± 0.13	1.96	3.7 ± 0.4	2.5
C337/C344	−	17.4 ± 4.2	1.10 ± 0.09	1.63	3.8 ± 0.5	1.8
	+	18.6 ± 3.7	0.66 ± 0.02	0.85	2.5 ± 0.4	1.7
	+DTT	18.0 ± 3.6	1.16 ± 0.16	1.77	4.0 ± 0.7	1.8

Single molecule motility assays for kinesin–GFP along sea urchin axonemes were performed using a total internal reflection microscope as described in the Materials and Methods.
* Disulfide bond was formed by oxidative treatment of the constructs with 200 μM DTNB (+). Disulfide formation was reversed by subsequent treatment with 5 mM DTT (+DTT). − indicates control reaction without DTNB. NEM indicates thiol-modification with 1 mM NEM.
[‡] Mean ± SD values were derived from >100 measurements of fluorescent spots. Mean velocities of C334/C222 and C330/C4 after DTNB treatment were obtained by dividing the average run length by average association time of the spots that were used to determine the run length (see below).
[§] Average run length was derived from fitting of the distribution as described in Materials and Methods. For C334/C222 and C330/C4 with DTNB, only the spots remained on the axonemes more than 0.5 s were used to obtain distributions. Errors of the fit are shown. Run lengths were corrected to account for the photobleaching rate of GFP: 0.086 s^{-1} at 5 mW laser power (Shimizu et al., 2000; Thorn et al., 2000). Distributions and fitting curves are shown in Figs. 2 b and 4 b.
[‖] Average association time was derived from the fit as described in Materials and Methods.
[¶] Frequencies of movement/binding of GFP spots on the axonemes were derived from >100 events normalized by observation time, length of the axoneme, and kinesin concentration.

ments (Fig. 2 b). Moreover, the MSD plot was nonlinear and was fitted well with a theoretical curve for Brownian diffusion (diffusion coefficient of 2.6×10^{-11} cm^2/s) superimposed with directed movement with a velocity of 3.2 μm/min (Fig. 3 b). This velocity is similar to that displayed by cross-linked Cys330/Cys4 kinesin in the microtubule gliding assay (Fig. 2 a). Since the disulfide bond between residues 330 and 4 should only partially constrain the neck linker, these results suggest that partial movement of neck linker is sufficient for directionality.

Since oxidized Cys330/Cys4 showed some net directed motion, we also investigated whether it has the ability to move processively under the applied load of an optical trap (Svoboda and Block, 1994; Kojima et al., 1997; Coppin et al., 1997). Individual beads coated with WT kinesin were captured with an optical trap and brought into contact with an axoneme. The kinesin concentration was adjusted such that only about half of the beads exhibited movement (18 beads moved out of 30 beads tested). Under this condition, >98% of the observed bead movements are expected to be generated by a single kinesin molecule (Svoboda and Block, 1994). Under reducing conditions, beads coated with Cys330/Cys4 at the same density as WT kinesin showed a similar frequency of movement (14 beads moved out of 30 beads). However, after oxidation, the Cys330/Cys4-coated beads showed hardly any movement (1 out of 40 beads moved and did so with normal velocity. This movement event may have been caused by a noncross-linked motor). Binding events oc-

curred for some beads, as suggested by a decrease in the thermal fluctuations of the beads in the trap (i.e., increase in stiffness due to the formation of the linkage between the bead and the microtubule). When the motor density was increased by 10-fold, movement of beads coated with oxidized Cys330/Cys4 were observed (11 out of 16 beads moved). Even under these multiple motor conditions, the force–velocity curve still was shifted to lower forces and the dissociation rate was increased compared with single molecule conditions of noncross-linked Cys330/Cys4 (Fig. 2 c; note that measurements were made with a fixed optical and not a force clamp apparatus; Therefore, the load is continually increasing as the bead moves away from the trap center). These results indicate that the cross-linked Cys330/Cys4 molecule exhibits impaired force production and processivity. In contrast, beads coated with oxidized Cys344/Cys222 did not show any movement even at the 10-fold higher motor density, confirming that oxidized Cys344/Cys222 has no or extremely limited motile activity.

Cross-linking of the Neck Coiled-Coil

To examine the effects of cross-linking of kinesin's neck coiled-coil, we introduced single cysteine residues into the *a* position of the first two heptad repeats (Fig. 1 a). This position is preferred for disulfide bond formation (Zhou et al., 1993) and also scored well for bond formation with the SS-BOND prediction program. We prepared three constructs by replacing Ala344, Tyr337, or Ala337/Tyr344 (double mutation) with cysteine(s). The residue 337 is the first residue
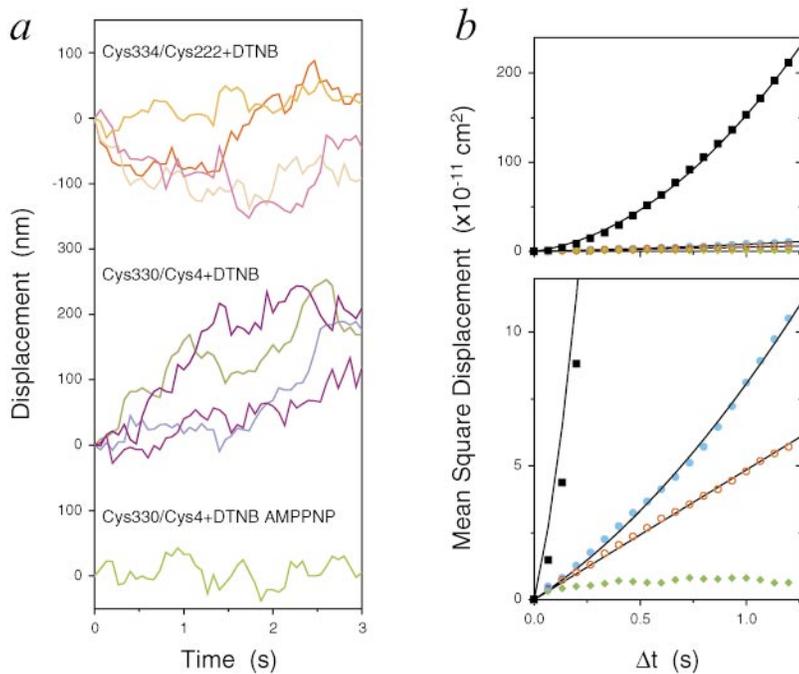
Figure 3. Diffusional motion of neck linker-cross-linked kinesin molecules. (a) Typical displacement plots for cross-linked Cys334/Cys222 and Cys330/Cys4. Y axis indicates the displacement toward plus end of axonemes. The polarity was determined by the direction of continuous motion of occasional noncross-linked molecules in the preparation. The variation in the position of cross-linked Cys330/Cys4 with the nonhydrolyzable ATP analogue AMPPNP (1 mM) reflects the error in the tracking of single molecules and not actual motion. (b) MSD plots for Cys334/Cys222 with DTNB (red circle), Cys330/Cys4 without DTNB (square), with DTNB (blue circle), with DTNB in the presence of 1 mM AMPPNP (diamond), as shown with two different magnifications in y axis. Lines show theoretical curves. Cys334/Cys222+DTNB was fitted with MSD = $2Dt$ ($D = 2.4 \times 10^{-11}$ cm²/s), and Cys330/Cys4 and Cys330/Cys4+DTNB were fitted with MSD = $2Dt + v^2t^2$ ($D = 17 \times 10^{-11}$ and 2.6×10^{-11} cm²/s and $v = 21$ and 3.2 μm/min, respectively; diffusion coefficient for Cys330/Cys4 without DTNB is overestimated due to the lack of temporal resolution). See supplemental videos 1 and 2, showing movements of Cys330/Cys4 without and with DTNB.

of the neck coiled-coil, and cross-linking at this position should completely inhibit unwinding of this structure. Residue 344 is located at the beginning of the second heptad repeat, and the disulfide bond formation at this position should only allow limited unwinding of the neck coiled-coil.

Disulfide bond formation induced by DTNB was evaluated using SDS-PAGE under nonreducing conditions (Fig. 1 c). After DTNB treatment, all neck coiled-coil mutants showed a high molecular weight band corresponding approximately in size to a cross-linked kinesin dimer (Fig. 1 c). The cross-linking efficiency was higher for Cys344 (65–90%) and Cys337/Cys344 (70–90%) than for Cys337 (55–75%). Subsequent treatment of the oxidized kinesin mutants with excess DTT completely reversed the cross-linking reaction (Fig. 1 c). WT was not affected by the oxidative treatment, which certifies that cross-linking requires the introduced mutations.

The effect of cross-linking within kinesin's neck coiled-coil was examined using the same assays described above for the neck linker mutations. Under reducing conditions, the above mutations did not themselves significantly affect kinesin ATPase activity, multiple motor microtubule gliding velocity, or single molecule velocity and processivity (Tables I and II). Furthermore, oxidative treatment produced only subtle effects on activity. For the microtubule-stimulated ATPase, the turnover rate was unchanged and the K_m(MT) slightly increased (Table I). However, this increase was also observed for the WT kinesin after oxidation, and thus, the increase in K_m(MT) may be caused by an effect of DTNB on the microtubule and not on the kinesin molecule. After DTNB treatment, microtubule gliding velocity decreased slightly (8%, 30%, and 17% for Cys344, Cys337, and Cys337/Cys344, respectively; Fig. 4 a and Table I). These effects are significantly smaller than those observed for neck linker mutants Cys334/Cys222 and Cys330/Cys4 (Fig. 2 a and Table I).

The effect of neck coiled-coil cross-linking on kinesin processivity was examined using single molecule motility assays. For all three neck coiled-coil mutants, the single molecule velocity was unchanged after DTNB-induced oxidation (Table II). The run lengths, however, decreased slightly (27%, 43%, and 48% for Cys344, Cys337, and Cys337/Cys344, respectively) (Fig. 4 b and Table II). The decreases in run length were completely recovered by subsequent treatments with excess DTT (Table II, +DTT), indicating that they were caused by cross-linking of the neck coiled-coil. Since the cross-linking was not 100% efficient (Fig. 1 c), one concern is that noncross-linked molecules could have been selectively observed in this assay. However, this possibility was excluded by the finding that the movement frequency of all mutants did not change after the DTNB treatment (Table II). Collectively, these results suggest that cross-linking of neck coiled-coil has minimal effect on motor activity, although it produces a slight decrease in single molecule run length.

To examine force production after neck coiled-coil cross-linking, optical trapping bead assays were performed. Beads coated with Cys337/Cys344 mutants were randomly trapped and attached onto axonemes. The movement frequency of beads did not change after DTNB treatment (25 out of 40 beads moved without DTNB and 21 out of 40 beads moved with DTNB). This result reveals that the microtubule binding frequency of this kinesin mutant does not change after oxidation, confirming the results from single molecule fluorescence assays. The force–velocity curve also was not significantly altered after oxidation (Fig. 4 c). However, after oxidation, the dissociation rate increased by ~1.6-fold at most loads (Fig. 4 c). This is consistent with the 1.5-fold increase in the dissociation rate (inverse of association time) observed in single molecule motility assays (Table II). The increase in the dissociation rate after oxidation was small and insignificant for the Cys344 mutant (Fig. 4 c).
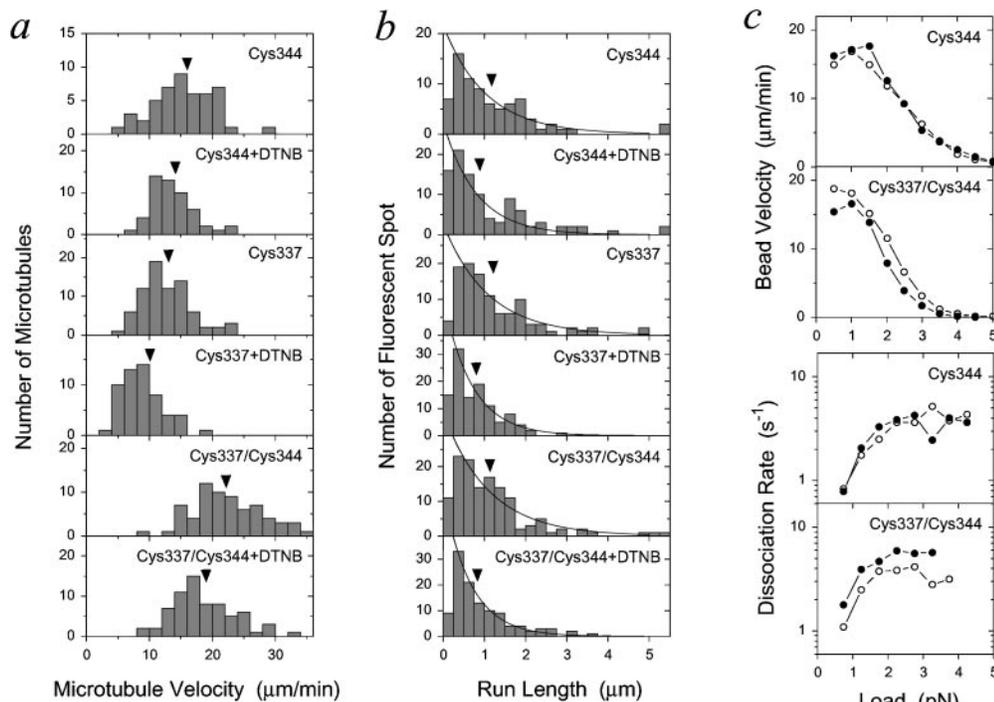
Figure 4. Effects of neck coiled-coil cross-linking on kinesin motility. (a) Histograms of microtubule gliding velocities without and with DTNB treatment are shown. Arrowheads indicate mean value (Table I). (b) Histograms of run lengths of single molecule motility of neck coiled-coil cross-linked kinesins along axonemes visualized using total internal reflection fluorescent microscopy. The run lengths were fit with an exponential curve. Arrowheads indicate average run length (Table II). (c) Load-dependent velocity and dissociation rate of Cys344 and Cys337/344 molecules were determined by optical trapping bead assays. (Open circle) Without DTNB; (closed circle) with DTNB. The increase in dissociation rate of Cys337/344 is statistically significant at lower forces, as tested by *t* test using dissociation rates obtained from 10 individual beads (*P* value of 0.018 and 0.015 at 0.75 and 1.25 pN, respectively). The increase in the dissociation rate of Cys344 was small (∼1.2-fold) and was not statistically significant at any load (*P* value of >0.3).

Forced Unwinding of the Neck Coiled-Coil Using Long Cross-linkers

We also examined whether the neck coiled-coil could be cross-linked using long cross-linkers and whether this forced unwinding of the coiled-coil affected motility. Two rigid bifunctional thiol reagent were employed (Fig. 5 a): *N,N'*-1,2-phenylenedimaleimide (oPDM) which spans two cysteine residues by 4–9 Å (compare to the sulfur–sulfur distance in a disulfide bond, which is 2 Å) and *N,N'*-1,4-phenylenedimaleimide (pPDM), which spans by 12–13 Å. Cys337 (as well as the Cys337/Cys344 mutant; not shown) was partially cross-linked by both oPDM and pPDM, as judged by the gel shift assay (Fig. 5 b). In contrast, Cys344 was not cross-linked by either agent (Fig. 5 b). Since the long bifunctional reagents cannot access position 344 in the neck coiled-coil, these results indicate that the structure is stable at this position. In contrast, the beginning of the coiled-coil at residue 337 is less stable, and can unwind at least transiently to permit access to the long cross-linker agents.

To determine how unwinding of the beginning of the coiled-coil affects kinesin function, we examined processive motion of Cys337 before and after cross-linking by oPDM or pPDM using the single molecule fluorescence motility assay. Cys337 mutants moved unidirectionally after oPDM or pPDM cross-linking, and the mean run lengths decreased by only 20% and 22%, respectively (corrected run length of 1.21 and 1.18 μm). The decrease in run length was less than that observed after DTNB treatment of Cys337 (Table II), possibly because the efficiency of cross-linking with oPDM and pPDM was lower that that with DTNB. The velocity of Cys337 motion was not affected by cross-linking with oPDM (19.1 ± 4.4 and

19.3 ± 4.4 μm/min for reduced and cross-linked respectively, *P* value of 0.8), but was significantly decreased after cross-linking with the longer cross-linker pPDM (15.3 ± 4.9 μm/min; *P* value of 0.00004) (Fig. 5 *c*). A decrease in velocity was also observed for Cys337/Cys344 after cross-linking with pPDM (20.1 ± 3.5 and 15.4 ± 5.7 μm/min for reduced and cross-linked, respectively, *P* value of 10^{-9}). The single molecule velocity for Cys344 was unchanged after treatment with pPDM (19.5 ± 3.5 and 20.3 ± 4.1 μm/min for reduced and cross-linked, respectively), which was expected since this reagent failed to cross-link this cysteine position. These results indicate that kinesin can move processively when the beginning of the neck coiled-coil is forced into an unwound configuration by cross-linking. However, in contrast to results for cross-linking into a closed state with DTNB, unwinding of the first heptad reduces the velocity of movement.

Discussion

Conformational Changes in the Neck Linker Are Essential for Motility

We have explored the neck linker's role in processive movement by preventing the neck linker movements using site-directed chemical cross-linking. Disulfide cross-linking of the neck linker at the tip of the catalytic core (Cys334/Cys222), which should prevent the unzipping of neck linker during the enzymatic cycle, resulted in a complete loss of unidirectional motion. Rice et al. (1999) previously documented that the neck linker is unzipped in nucleotide-free and ADP states, and zippered after microtubule-docked kinesin binds ATP. These findings were obtained in a truncated, monomeric kinesin, but it was hy-
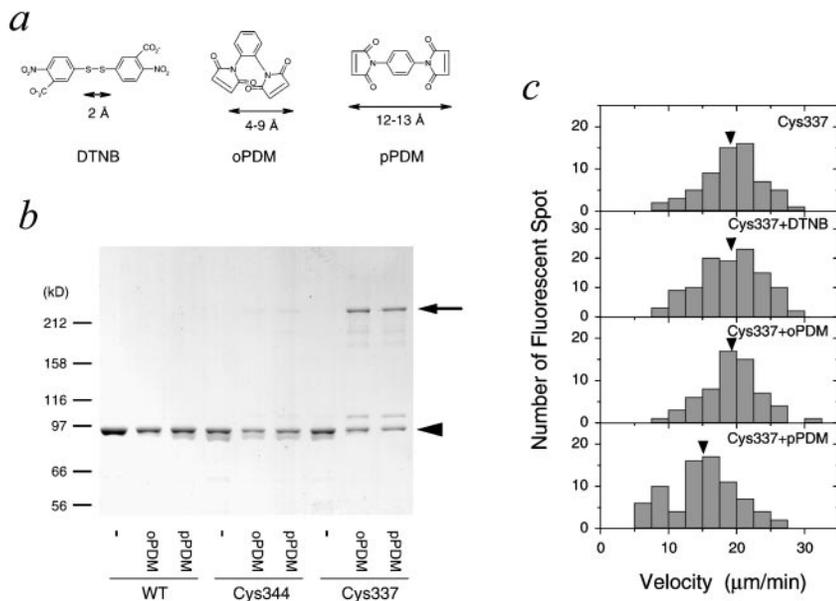
Figure 5. Cross-linking of the neck coiled-coil using long cross-linkers. (a) Structures of the cross-linking agents oPDM and pPDM possessing two maleimide groups that react with thiols. (b) Cross-linking of neck coiled-coil mutants Cys344 and Cys337 using oPDM or pPDM analyzed by SDS-PAGE. Arrowhead and arrow show noncross-linked and cross-linked kinesin, respectively. The concentration of cross-linking agent was 100 μM. (c) Histogram of velocities of Cys337 after cross-linking, analyzed using the single molecule fluorescence motility assays. The arrows denote the mean velocities (19.1 ± 4.4, 19.4 ± 4.4, 19.3 ± 4.4 and 15.3 ± 4.9 μm/min for reduced-, with DTNB-, oPDM-, and pPDM-treated, respectively). The shift in the distribution after cross-linking with pPDM most likely reflects the presence of both cross-linked and noncross-linked molecules.

pothesized that the neck linker conformational changes are essential for processivity in the kinesin dimer. Specifically, rezippering reaction of neck linker in the forward head in the microtubule-bound kinesin dimer would be expected to propel the rear kinesin head to a forward tubulin binding site along the microtubule (Fig. 6 a) (see also animated movie from Vale and Milligan, 2000; www.sciencemag.org/feature/data/1049155.shl). The loss of kinesin dimer motility after neck linker cross-linking to the catalytic core provides strong support for this model.

In contrast to the ablation of motility by cross-linking of Cys334/Cys222, cross-linking the middle of the neck linker (Cys330) to the very NH₂ terminus (Cys4) still permitted limited directional motion of the kinesin dimer. Since the COOH-terminal end of neck linker could still unzipper/rezipper in this cross-linked molecule in response to nucleotide-dependent motions of a critical "relay" (or "switch II") helix (Vale and Milligan, 2000), this result suggests that a partial movement of the neck linker can elicit directional movement. However, the motion in the oxidized Cys330/Cys4 kinesin dimer is very slow (microtubule velocity of 2.5 μm/min) and comparable to the velocity generated by truncated kinesin monomers (2.4 μm/min; Rice et al., 1999). Moreover, in single molecule assays, the oxidized Cys330/Cys4 kinesin dimer showed biased diffusion instead of normal unidirectional processivity and was severely compromised in pulling against a load in the optical trap. These results indicate that limited neck linker mobility compromises the formation of a two-head–bound intermediate, which is thought to be essential for kinesin processivity and force production (Fig. 6 b). The twofold decrease in microtubule-stimulated ATP-turnover rate after oxidative cross-linking also is consistent with the failure of the dimeric motor to form a two-head–bound intermediate on the microtubule (Hackney, 1994). According to the mechanically controlled access model (Vale and Milligan, 2000), contact of both heads with the microtubule requires that the neck linker be completely zippered in the rear head and unzippered in the forward head. Since the latter reaction is inhibited by neck linker cross-linking, only one head will have its ATPase cycle stimulated when

the kinesin dimer encounters a microtubule (Fig. 6, b and c). Thus, results from the single molecule fluorescence processivity assay, force-generation studies with the optical trap, and the ATPase assays all are consistent with the proposed role of the neck linker in kinesin-generated movement.

Unwinding of the Neck Coiled-Coil Is Not Essential for Processive Movement

In contrast to the results obtained with neck linker cross-linking, disulfide cross-linking at the beginning of the neck coiled-coil (Cys337) or the beginning of the second heptad (Cys344) had little effect on motor function. These results are inconsistent with the proposal (Tripet et al., 1997; Hoenger et al., 2000) that the neck coiled-coil unwinds to around position 352 to allow the two kinesin heads to separate and form a two-head–bound intermediate on the microtubule. Instead, our results indicate that neck coiled-coil unwinding does not need to occur during processive motion. However, some of our data suggests that limited unwinding of the first heptad may occur and could play a minor role in processivity. Using long cross-linking reagents, we were able to form cross-links between cysteines at position 337 but not 344. Since the longer cross-linking agent (pPDM) can only cross-link cysteines separated by at least 10 Å, these results suggest that the neck coiled-coil of kinesin in solution must "breathe" around position 337 but not at 344. We also find that cross-linking at 337 increases the dissociation rate of the kinesin motor, leading to somewhat shorter run lengths. Unraveling of the first few residues of the neck coiled-coil could aid in the formation of the two-head–bound intermediate, thereby reducing the probability of detachment from a one-head–bound state (see also accompanying paper by Thorn et al., 2000).

Two published reports also have examined the effects of stabilizing kinesin's neck coiled-coil. Romberg et al. (1998) replaced the majority of the neck coiled-coil (residues 343–370) with a highly stable artificial coiled-coil (over twofold more stable than kinesin's endogenous coiled coil; Tripet et al., 1997) and reported a small decrease in run length
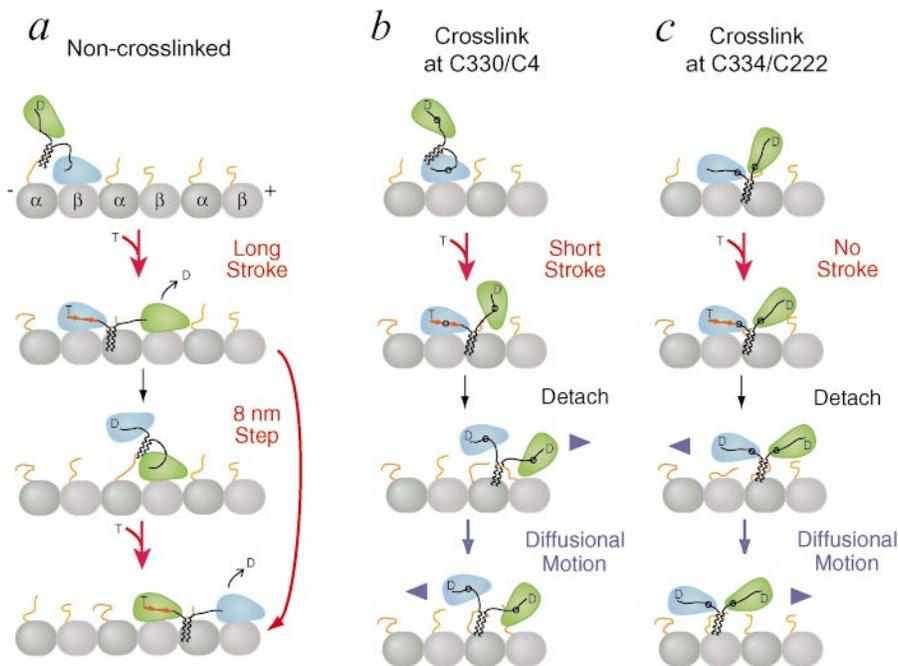
Figure 6. Schematic model showing the effects of neck linker cross-linking on kinesin movement. Two kinesin's catalytic cores are shown in blue and green, and the adjacent neck linker and the neck coiled-coil are shown in black lines. α- and β-tubulin subunits are shown in gray with the flexible COOH terminus region shown by an orange line. T and D denote ATP and ADP, respectively. (a) Model for processive movement of kinesin as described previously (Rice et al., 1999; Vale and Milligan, 2000). Upon binding of ATP to the microtubule-bound head, the neck linker docks onto the catalytic core and moves partner head toward plus end. The forward head searches and binds to a new tubulin-binding site to achieve two-head–bound intermediate. Kinesin can repeat this cycle more than 100 times before detachment from the microtubule. (b) Cross-linking of the neck linker at the middle (Cys330/Cys4) enables directional motion due to a small power stroke but not processive motion. Upon binding of ATP, a part of the neck linker in the microtubule-bound head folds (red arrows). However, the access of the partner head to a tubulin-binding site is inhibited until the bound head detaches. The motor partitions between a weak binding state in which it can diffuse along the microtubule and a strong binding state in which it can undergo a short stroke. (c) Disulfide cross-linking of the neck linker at the tip of the catalytic core (Cys334/Cys222) abolishes motile activity, since the neck linker cannot change position. Weak electrostatic interaction between the COOH terminus of tubulin and the initial portion of the neck coiled-coil allows the molecule to diffuse along the microtubule (see also Thorn et al., 2000).

(45% decrease) with no change in velocity. Replacing the entire coiled coil (residues 337–370) yielded similar results (46% decrease in run length and no change in velocity) (Ubersax, J., Thorn, K., and Vale, R., unpublished results). These results have been criticized on the basis that they do not exclude a partial unwinding of this stable coiled-coil structure (Mandelkow and Hoenger, 1999). These previous results, however, are consistent with those obtained here with cross-linking of the neck coiled-coil at Cys337 or Cys337/Cys344 (43% and 48% decrease in run length, respectively; no change in velocity, Table II). Hoenger et al. (2000) also created similar construct to our Cys337 mutant, although they introduced this cysteine in a wild type rat kinesin dimer that contained other solvent-exposed cysteine residues. They reported no difference in the structure of the kinesin-microtubule complex by cryo-EM, and suggested that the cross-linked kinesin can still form a two-head–bound intermediate. However, they noted an unusual stabilization and curvature of cross-linked kinesin-decorated microtubule protofilaments in the axial direction, suggesting that a strain was imposed on the protofilament by the kinesin. Hoenger also reported a 13-fold decrease in K_m(MT) after oxidization, which they interpreted as indicative of a substantial decrease in processivity. However, this decrease in K_m(MT) is inconsistent with our results (Table I), and raises the possibility that oxidation of other solvent-exposed cysteines caused the increase in K_m(MT) in their construct (Walker et al., 1997).

In summary, our results confirm that the unwinding of the neck coiled-coil is not involved in coordinated movement of kinesin dimer. Rather, integrity of the neck coiled-coil is likely to be important for this process, as it constrains the neck linkers of the two kinesin heads to adopt opposite conformations in the two-head–bound intermediate state. Furthermore, strain built up at the two-head–bound intermediate is thought to be important for such coordination between the two heads (i.e., for a mechanical action in the forward neck linker to be communicated to the rear head). In further support of this idea, we show here that forced unwinding of the beginning of the coiled-coil with long cross-linkers decreases movement velocity, and introduction of a flexible glycine linker at the beginning of the neck coiled-coil also impairs processivity (Romberg et al., 1998; Jiang, W., J.-Q. Cheng, J. Moore, R. Patterson, M.F. Stock, and D.D. Hackney. 1999. *Biophys. J.* 76:A17).

Although not undergoing a major conformational change, the neck coiled-coil is likely to play an important modulatory role in processivity. In the accompanying paper, Thorn et al. (2000) show that the kinesin run length can be affected by a weak electrostatic interaction occurring between the neck coiled-coil and the COOH-terminal region of tubulin. One possible explanation for the decrease in processivity after 337 cross-linking is that it impairs the binding interaction of the neck coiled-coil with the COOH terminus of tubulin.

Diffusional Motions of Cross-linked Kinesin Dimers along Microtubules

An unexpected result from our experiments was the finding that neck linker cross-linking causes kinesin to undergo one-dimensional diffusion along the microtubule. Interestingly, the diffusion coefficient for motion that we measured ($\sim 2.5 \times 10^{-11}$ cm^2/s) is similar to a diffusion coefficient estimated from the fluctuation analysis of optical trapping data of processive kinesin dimer (Svoboda et al., 1994; Imafuku et al., 1996). This suggests that diffusion is

an intrinsic property of a kinesin dimer, and becomes clearly evident only after the conformational change that produces unidirectional movement is impaired by neck linker cross-linking. This diffusion phenomenon may again involve a weak electrostatic interaction between the COOH terminus of tubulin and the neck coiled-coil, since neck linker cross-linking of a monomeric construct (Cys330/Cys4 in Cys-light K339) did not elicit detectable diffusional movement (i.e., single motors bound and dissociated rapidly) (data not shown).

The biased one-dimensional diffusion observed for cross-linked Cys330/Cys4 is reminiscent of a similar phenomenon described for a KIF1A chimera (catalytic core of the kinesin-related protein KIF1A and the neck linker of conventional kinesin) (Okada and Hirokawa, 1999, 2000). Oxidized Cys330/Cys4, however, shows a 17-fold lower diffusion rate than the KIF1A chimera, which may reflect a difference in their duty ratios (ratio of tight and weak binding state) (Howard, 1997). Supporting this idea, the diffusion coefficient of oxidized Cys330/Cys4 in the weak binding state (in the presence of 1 mM ADP) increased eightfold (2.2×10^{-10} cm^2/s) and became more similar to the KIF1A chimera (4.4×10^{-10} cm^2/s) (data not shown). We also find that the biased diffusional motion of oxidized Cys330/Cys4 is unable to generate much work against a load. Whether the same is true for the KIF1A chimera has not been addressed.

The molecular basis of biased diffusional motion is still unclear, and it is also uncertain whether the motions of oxidized Cys330/Cys4 and the KIF1A chimera reflect similar or different mechanisms. In both cases, however, it appears as though these two motor proteins have mechanisms for maintaining a weak interaction with the COOH terminus of tubulin (through the lysine-rich L12 loop for KIF1A [Okada and Hirokawa, 2000; Kikkawa et al., 2000] and the neck coiled-coil for kinesin [Thorn et al., 2000]), which allows them to diffuse randomly along the microtubule when the heads are in their weak binding ADP state (Fig. 6 b). Since the COOH terminus of tubulin is likely to be flexible and mobile, motors may be able to diffuse along microtubules by transferring rapidly from the COOH terminus of one subunit to the COOH terminus of an adjacent subunit. Two mechanisms could create an ATP-dependent bias to this diffusion (Okada and Hirokawa, 1999): (a) through an asymmetry in the binding potential of the motor–microtubule interaction; or (b) through a conformational change in the motor that biases its subsequent attachment to a tubulin in one direction. We favor the latter model, since oxidized Cys334/Cys222, which has normal ATPase activity but cannot undergo the neck linker conformational change, does not display biased diffusion in the presence of the ATP. In the case of oxidized Cys330/Cys4, we propose that the limited neck linker conformational change shifts the probability of a subsequent motor attachment to the tubulin subunit towards the plus-end. By this mechanism, the motor could undergo a net directional motion through repeated attachment, power stroke, and detachment reactions (Fig. 6 b).

References

Block, S.M. 1998. Kinesin: what gives? *Cell.* 93:5–8.

Block, S.M., L.S.B. Goldstein, and B.J. Schnapp. 1990. Bead movement by single kinesin molecules studied with optical tweezers. *Nature.* 348:348–352.

Case, R.B., D.W. Pierce, N. Hom-Booher, C.L. Hart, and R.D. Vale. 1997. The directional preference of kinesin motors is specified by an element outside of the motor catalytic domain. *Cell.* 90:959–966.

Case, R.B., S. Rice, C.L. Hart, B. Ly, and R.D. Vale. 2000. Role of the kinesin neck linker and catalytic core in microtubule-based motility. *Curr. Biol.* 10:157–160.

Chandrasekhar, S. 1943. Stochastic problems in physics and astronomy. *Rev. Mod. Phys.* 15:1–89.

Coppin, C.M., D.W. Pierce, L. Hsu, and R.D. Vale. 1997. The load dependence of kinesin's mechanical cycle. *Proc. Natl. Acad. Sci. USA.* 94:8539–8544.

Endow, S.A., and H. Higuchi. 2000. A mutant of the motor protein kinesin that moves in both directions on microtubules. *Nature.* 406:913–916.

Gilbert, S.P., M.L. Moyer, and K.A. Johnson. 1998. Alternating site mechanism of the kinesin ATPase. *Biochemistry.* 37:792–799.

Gittes, F., E. Meyhofer, S. Baek, and J. Howard. 1996. Directional loading of the kinesin motor molecule as it buckles a microtubule. *Biophys. J.* 70:418–429.

Goldstein, L.S.B., and A.V. Philp. 1999. The load less traveled: emerging principles of kinesin motor utilization. *Annu. Rev. Cell Dev. Biol.* 15:141–183.

Hackney, D.D. 1994. Evidence for alternating head catalysis by kinesin during microtubule-stimulated ATP hydrolysis. *Proc. Natl. Acad. Sci. USA.* 91:6865–6869.

Hackney, D.D. 1995. Highly processive microtubule-stimulated ATP hydrolysis by dimeric kinesin head domains. *Nature.* 377:448–450.

Hazes, B., and B.W. Dijkstra. 1988. Model building of disulfide bonds in proteins with known three-dimensional structure. *Protein Engineering.* 2:119–125.

Hirokawa, N. 1998. Kinesin and dynein superfamily proteins and the mechanism of organelle transport. *Science.* 279:519–526.

Hoenger, A., S. Sack, M. Thormahlen, A. Marx, J. Muller, H. Gross, and E. Mandelkow. 1998. Image reconstructions of microtubules decorated with monomeric and dimeric kinesins: comparison with X-ray structure and implications for motility. *J. Cell Biol.* 141:419–430.

Hoenger, A., M. Thormahlen, R. Diaz-Avalos, M. Doerhoefer, K.N. Goldie, J. Muller, and E. Mandelkow. 2000. A new look at the microtubule binding patterns of dimeric kinesins. *J. Mol. Biol.* 297:1087–1103.

Howard, J. 1997. Molecular motors: structural adaptations to cellular functions. *Nature.* 389:561–567.

Howard, J., A.J. Hudspeth, and R.D. Vale. 1989. Movement of microtubules by single kinesin molecules. *Nature.* 342:154–158.

Imafuku, Y., Y.Y. Toyoshima, and K. Tawada. 1996. Fluctuation in the microtubule sliding movement driven by kinesin in vitro. *Biophys. J.* 70:878–886.

Kikkawa, M., Y. Okada, and N. Hirokawa. 2000. 15 Å resolution model of the monomeric kinesin motor, KIF1A. *Cell.* 100:241–252.

Kojima, H., E. Muto, H. Higuchi, and T. Yanagida. 1997. Mechanics of single kinesin molecules measured by optical trapping nanometry. *Biophys. J.* 73:2012–2022.

Kozielski, F., S. Sack, A. Marx, M. Thormahlen, E. Schonbrunn, V. Biou, A. Thompson, E.-M. Mandelkow, and E. Mandelkow. 1997. The crystal structure of dimeric kinesin and implications for microtubule-dependent motility. *Cell.* 91:985–994.

Kull, F.J., E.P. Sablin, R. Lau, R.J. Fletterick, and R.D. Vale. 1996. Crystal structure of the kinesin motor domain reveals a structural similarity to myosin. *Nature.* 380:550–555.

Mandelkow, E., and K.A. Johnson. 1998. The structural and mechanochemical cycle of kinesin. *Trends Biochem. Sci.* 23:429–433.

Mandelkow, E., and A. Hoenger. 1999. Structures of kinesin and kinesin-microtubule interactions. *Curr. Opin. Cell Biol.* 11:34–44.

Okada, Y., and N. Hirokawa. 1999. A processive single-headed motor: kinesin superfamily protein KIF1A. *Science.* 283:1152–1157.

Okada, Y., and N. Hirokawa. 2000. Mechanism of the single-headed processivity: diffusional anchoring between the K-loop of kinesin and the C terminus of tubulin. *Proc. Natl. Acad. Sci. USA.* 97:640–645.

Pierce, D.W., and R.D. Vale. 1998. Assaying processive movement of kinesin by fluorescence microscopy. *Methods Enzymol.* 298:154–171.

Pierce, D.W., and R.D. Vale. 1999. Single-molecule fluorescence detection of green fluorescence protein and application to single-protein dynamics. *Methods Cell Biol.* 58:49–73.

Rice, S., A.W. Lin, D. Safer, C.L. Hart, N. Naber, B.O. Carragher, S.M. Cain, E. Pechatnikova, E.M. Wilson-Kubalek, M. Whittaker, et al. 1999. A structural change in the kinesin motor protein that drives motility. *Nature.* 402:778–784.

Romberg, L., D.W. Pierce, and R.D. Vale. 1998. Role of the kinesin neck region in processive microtubule-based motility. *J. Cell Biol.* 140:1407–1416.

Sack, S., J. Muller, A. Marx, M. Thormahlen, E.M. Mandelkow, S.T. Brady, and E. Mandelkow. 1997. X-ray structure of motor and neck domains from rat brain kinesin. *Biochemistry*. 36:16155–16165.

Shimizu, T., K.S. Thorn, A. Ruby, and R.D. Vale. 2000. ATPase kinetics characterization and single molecule behavior of mutant human kinesin motors defective in microtubule-based motility. *Biochemistry*. 39:5265–5273.

Svoboda, K., and S.M. Block. 1994. Force and velocity measured for single kinesin molecules. *Cell*. 77:773–784.

Svoboda, K., C.F. Schmidt, B.J. Schnapp, and S.M. Block. 1993. Direct observation of kinesin stepping by optical trapping interferometry. *Nature*. 365:721–727.

Svoboda, K., P.P. Mitra, and S.M. Block. 1994. Fluctuation analysis of motor protein movement and single enzyme kinetics. *Proc. Natl. Acad. Sci. USA*. 91:11782–11786.

Thormahlen, M., A. Marx, S. Sack, and E. Mandelkow. 1998. The coiled-coil helix in the neck of kinesin. *J. Struct. Biol*. 122:30–41.

Thorn, K.S., J.A. Ubersax, and R.D. Vale. 2000. Engineering the processive run length of the kinesin motor. *J. Cell Biol*. 151:1093–1100.

Tripet, B., R.D. Vale, and R.S. Hodges. 1997. Demonstration of coiled-coil interactions within the kinesin neck region using synthetic peptides: implications for motor activity. *J. Biol. Chem*. 272:8946–8956.

Vale, R.D., and R.J. Fletterick. 1997. The design plan of kinesin motors. *Annu. Rev. Cell. Dev. Biol*. 13:745–777.

Vale, R.D., and R.A. Milligan. 2000. The way things move: looking under the hood of molecular motor proteins. *Science*. 288:88–95.

Vale, R.D., T. Funatsu, D.W. Pierce, L. Romberg, Y. Harada, and T. Yanagida. 1996. Direct observation of single kinesin molecules moving along microtubules. *Nature*. 380:451–453.

Vale, R.D., D.R. Soll, and I.R. Gibbons. 1989. One-dimensional diffusion of microtubules bound to flagellar dynein. *Cell*. 59:915–925.

Walker, R.A., E.T. O'Brien, D.L. Epstein, and M.P. Sheetz. 1997. n-ethylmaleimide and ethacrynic acid inhibit kinesin binding to microtubules in a motility assay. *Cell Motil. Cytoskeleton*. 37:289–299.

Woehlke, G., A.K. Ruby, C.L. Hart, B. Ly, N. Hom-Booher, and R.D. Vale. 1997. Microtubule interaction site of the kinesin motor. *Cell*. 90:207–216.

Zhou, N.E., C.M. Kay, and R.S. Hodges. 1993. Disulfide bond contribution to protein stability: positional effects of substitution in the hydrophobic core of the two-stranded α-helical coiled-coil. *Biochemistry*. 32:3178–3187.